The final publication is available at

http://dx.doi.org/10.1364/OE.22.028584

Time and frequency pump-probe multiplexing to enhance the signal response of Brillouin optical time-domain analyzers

Marcelo A. Soto,[1,*] Amelia Lavinia Ricchiuti,[2] Liang Zhang,[1,†] David Barrera,[2] Salvador Sales,[2] and Luc Thévenaz[1]

[1]EPFL Swiss Federal Institute of Technology, Institute of Electrical Engineering, SCI STI LT, Station 11, CH-1015 Lausanne, Switzerland
[2]ITEAM Research Institute, Universidad Politécnica de Valencia, Camino de Vera s/n, 46022 Valencia, Spain
[†] Permanent address: Department of Physics and Astronomy, State Key Lab of Advanced Optical Communication Systems and Networks, Shanghai Jiao Tong University, 200240 Shanghai, China
[*]marcelo.soto@epfl.ch

Abstract: A technique to enhance the response and performance of Brillouin distributed fiber sensors is proposed and experimentally validated. The method consists in creating a multi-frequency pump pulse interacting with a matching multi-frequency continuous-wave probe. To avoid nonlinear cross-interaction between spectral lines, the method requires that the distinct pump pulse components and temporal traces reaching the photo-detector are subject to wavelength-selective delaying. This way the total pump and probe powers launched into the fiber can be incrementally boosted beyond the thresholds imposed by nonlinear effects. As a consequence of the multiplied pump-probe Brillouin interactions occurring along the fiber, the sensor response can be enhanced in exact proportion to the number of spectral components. The method is experimentally validated in a 50 km-long distributed optical fiber sensor augmented to 3 pump-probe spectral pairs, demonstrating a signal-to-noise ratio enhancement of 4.8 dB.

References and links

1. T. Horiguchi, K. Shimizu, T. Kurashima, M. Tateda, and Y. Koyamada, "Development of a distributed sensing technique using Brillouin scattering," J. Lightwave Technol. **13**(7), 1296-1302 (1995).
2. M. A. Soto, and L. Thévenaz, "Modeling and evaluating the performance of Brillouin distributed optical fiber sensors," Opt. Express **21**(25), 31347-31366 (2013).
3. S. M. Foaleng, and L. Thévenaz, "Impact of Raman scattering and modulation instability on the performances of Brillouin sensors," Proc. SPIE **7753**, 77539V (2011).
4. M. Alem, M. A. Soto, and L. Thévenaz, "Modelling the depletion length induced by modulation instability in distributed optical fibre sensors," Proc. SPIE **9157**, 91575S (2014).
5. L. Thévenaz, S. Foaleng Mafang, and J. Lin, "Effect of pulse depletion in a Brillouin optical time-domain analysis system," Opt. Express **21**(12), 14017-14035 (2013).
6. A. Minardo, R. Bernini, L. Zeni, "A Simple Technique for Reducing Pump Depletion in Long-Range Distributed Brillouin Fiber Sensors," Sensors Journal, IEEE **9**(6), 633-634 (2009).
7. M. A. Soto, G. Bolognini, F. Di Pasquale, and L. Thévenaz, "Simplex-coded BOTDA fiber sensor with 1 m spatial resolution over a 50 km range," Opt. Lett. **35**(2), 259-261 (2010).
8. M. A. Soto, G. Bolognini, and F. Di Pasquale, "Analysis of pulse modulation format in coded BOTDA sensors," Opt. Express **18**(14), 14878-14892 (2010).
9. F. Rodriguez-Barrios, S. Martin-Lopez, A. Carrasco-Sanz, P. Corredera, J. D. Ania-Castanon, L. Thévenaz, and M. Gonzalez-Herraez, "Distributed Brillouin Fiber Sensor Assisted by First-Order Raman Amplification," J. Lightwave Technol. **28**(15), 2162-2172 (2010).
10. S. Martin-Lopez, M. Alcon-Camas, F. Rodriguez, P. Corredera, J. D. Ania-Castañón, L. Thévenaz, and M. Gonzalez-Herraez, "Brillouin optical time-domain analysis assisted by second-order Raman amplification," Opt. Express **18**(18), 18769-18778 (2010).

11. M. A. Soto, G. Bolognini, and F. Di Pasquale, "Optimization of long-range BOTDA sensors with high resolution using first-order bi-directional Raman amplification," Opt. Express **19**(5), 4444-4457 (2011).
12. M. A. Soto, G. Bolognini, and F. Di Pasquale, "Simplex-Coded BOTDA Sensor Over 120 km SMF with 1 m Spatial Resolution Assisted by Optimized Bidirectional Raman Amplification," IEEE Photon. Technol. Lett. **24**(20), 1823-1826 (2012).
13. X. Jia, Y. Rao, C. Yuan, J. Li, X. Yan, Z. Wang, W. Zhang, H. Wu, Y. Zhu, and F. Peng, "Hybrid distributed Raman amplification combining random fiber laser based 2nd-order and low-noise LD based 1st-order pumping," Opt. Express **21**(21), 24611-24619 (2013).
14. M. A. Soto, X. Angulo-Vinuesa, S. Martin-Lopez, S.-H. Chin, J. D. Ania-Castanon, P. Corredera, E. Rochat, M. Gonzalez-Herraez, and L. Thévenaz, "Extending the Real Remoteness of Long-Range Brillouin Optical Time-Domain Fiber Analyzers," J. Lightwave Technol. **32**(1), 152-162 (2014).
15. M. A. Soto, G. Bolognini, and F. Di Pasquale, "Distributed optical fibre sensors based on spontaneous Brillouin scattering employing multimode Fabry-Pérot lasers," Electr. Lett. **45**(21), 1071-1072 (2009).
16. C. Li, Y. Lu, X. Zhang, and F. Wang, "SNR enhancement in Brillouin optical time domain reflectometer using multi-wavelength coherent detection," Electr. Lett. **48**(18), 1139-1141 (2012).
17. A. Voskoboinik, J. Wang, B. Shamee, S. R. Nuccio, L. Zhang, M. Chitgarha, A. E. Willner, and M. Tur, "SBS-Based Fiber Optical Sensing Using Frequency-Domain Simultaneous Tone Interrogation," J. Lightwave Technol. **29**(11), 1729-1735 (2011).
18. A. Voskoboinik, O. Yilmaz, A. Willner, and M. Tur, "Sweep-free distributed Brillouin time-domain analyzer (SF-BOTDA)," Opt. Express **19**(26), B842-B847 (2011).
19. P. Chaube, B. G. Colpitts, D. Jagannathan, and A. W. Brown, "Distributed Fiber-Optic Sensor for Dynamic Strain Measurement," IEEE Sensors J. **8**(7), 1067-1072 (2008).
20. M. Nikles, L. Thévenaz, and P. A. Robert, "Brillouin gain spectrum characterization in single-mode optical fibers," J. Lightwave Technol. **15**(10), 1842-1851 (1997).
21. I. Jacobs, "Dependence of Optical Amplifier Noise Figure on Relative-Intensity-Noise," J. Lightwave Technol. **13**(7), 1461-1465 (1995).
22. M. A. Soto, and L. Thévenaz, "Towards 1'000'000 resolved points in a distributed optical fibre sensor," Proc. SPIE **9157**, 23rd International Conference on Optical Fibre Sensors OFS-23, 9157C3 (2014).
23. G. Bolognini, M. A. Soto, and F. Di Pasquale, "Fiber-Optic Distributed Sensor Based on Hybrid Raman and Brillouin Scattering Employing Multiwavelength Fabry-Pérot Lasers," IEEE Photon. Tech. Lett. **21**(20), 1523-1525 (2009).

1. Introduction

Impressive progresses in the development of Brillouin distributed optical fiber sensors have been reported during the past decade, turning this technology into one of the most interesting solutions to perform distributed strain and temperature monitoring over many tens of kilometers with a metric spatial resolution. One of the schemes that offers the highest sensing performance is called Brillouin optical-time domain analysis (BOTDA) [1], which is based on the interaction of a high-power pulsed pump and a counter-propagating continuous-wave (CW) probe signal through stimulated Brillouin scattering (SBS). The performance of the sensor is ultimately given by the signal-to-noise ratio (SNR) of the measurements, which is basically determined by the sensor amplitude response [2]. This response in turn depends on the input pump and probe powers, the spatial resolution and the total fiber attenuation, ultimately given by the fiber length [2]. It is therefore observed that for very long sensing ranges, the sensor response and the consequent SNR is significantly reduced, imposing a fundamental limitation to the sensor performance [2].

One of the main limitations on the sensor response in Brillouin sensing is related to the maximum pump power that can be launched into the sensing fiber, which eventually limits the available power near the distant fiber end. In particular, the pump pulse turns out to be depleted by the onset of nonlinearities, essentially by modulation instability (MI) [3,4], which limits the peak input pump power to about 100-150 mW in long standard single-mode fibers. An alternative to avoid modulation instability is propagating in fibers under normal dispersion ($D < 0$) at the pump wavelength, such as sufficiently dispersion-shifted fibers. However, in this kind of fibers the peak pump power cannot be raised indefinitely as well and is in turn depleted by forward amplified spontaneous Raman scattering, which imposes a power limit of ~600 mW [3]. The CW probe power turns out to be even more strictly limited to some ~5 mW by backward spontaneous Brillouin scattering amplified all along the fiber length. The probe should even be set to a much lower power to prevent a pronounced pump depletion that can

lead to significant gain spectral distortions [5]. However, this effect can be mitigated by using a 2-line probe performing a balanced gain-loss Brillouin interaction that massively compensates pump depletion in a small gain regime [5,6].

The power limits imposed on the pump and probe signals by nonlinear effects bind the best performance that an optimized sensor system can reach, giving rise to the well-known trade-off between spatial resolution and sensing distance range. Some methods have been recently proposed to partially overcome this trade-off and to extend the sensing range of Brillouin sensors, while maintaining a high spatial resolution. Essentially optical pulse coding [7,8] and distributed Raman amplification [9-11] can be used to enhance the Brillouin interaction along the sensing fiber, and consequently, to increase the optical power reaching the receiver. In particular, optical pulse coding methods employ pulse sequences to increase the total pump power launched into the sensing fiber; while the relevant signal is then retrieved by a post-processing procedure [7,8]. Additionally, high-power Raman pumping signals can be launched into the sensing fiber at a wavelength of ~1460 nm, so that they seamlessly amplify the Brillouin pump and probe signals during propagation along the fiber [9-11]. Significant performance improvements have been reported in the state-of-the-art, showing sensing ranges beyond 100 km when the two methods are combined in a single system [12-14].

In this paper an alternative technique is proposed and experimentally validated in order to further push the fundamental limits imposed by nonlinear effects. The method requires the generation of a pump and a probe signal distributed over multiple spectral components. Although the power of each frequency component is still limited by the onset of detrimental nonlinear effects, the total power launched into the sensing fiber can be considerably increased, exceeding the threshold of nonlinear effects as rated for individual signals, and thus leading to a significant enhancement in the sensor response. Additionally, a wavelength-dependent delay has to be applied to the pump to avoid nonlinear cross-interactions between the high-power pump spectral components. A proof-of-concept experiment is implemented based on two arrays of fiber Bragg gratings (FBGs), which deliver suitable delaying and filtering on the optical signals. Experimental results demonstrate the capability of the technique to upscale the sensor response improving the SNR of the measurements, while the limiting nonlinear effects are not observed in spite of increased pump and probe powers.

2. Proposed method based on a multi-frequency pump-probe Brillouin interaction

The technique proposed in this paper consists in creating a multi-frequency pump pulse interacting with a matching multi-frequency CW probe wave. It is important to mention that there have been some prior works using multi-tone signals to interrogate distributed Brillouin sensors [15-19]: for instance, the schemes described in [15,16] use a multi-wavelength optical pump to improve the performance of Brillouin optical time-domain reflectometers (BOTDR), while the method proposed in [17,18] makes use of multiple tones in a BOTDA system to eliminate the need for pump-probe frequency scanning and to make fast dynamic measurements possible. Although there are some similarities with the mentioned prior works [17-19], the implementation and objectives of the method proposed here are significantly different. Actually, the use of time and frequency pump-probe multiplexing in this case allows the total power launched into the fiber to be increased in order to push the limits imposed by nonlinear effects, resulting especially useful for long-range sensing schemes. This way, as it will be described later in the paper, the proposed method has allowed the first implementation of a long-range Brillouin sensor using 300 mW peak pump power without activating detrimental nonlinear effects, such as modulation instability. Contrarily to the method described in [17,18], in which two frequency combs having distinct frequency separations are used to interrogate different regions of the Brillouin gain spectrum, in the technique proposed here the interacting probe and pump spectral components have rigorously the same frequency spacing in order to multiply the response of the Brillouin interaction by a factor N (equal to the number of tones) at each scanned pump-probe frequency offset. This way a strong sensing response can be obtained, providing a significant SNR enhancement with respect to a standard

BOTDA scheme. Furthermore, the proposed technique is fully compatible with a simple direct detection, avoiding sophisticated coherent detection schemes, as needed in [15-19]; thus, requiring minimum changes to the conventional BOTDA scheme, since the frequency scan, acquisition procedure and data processing remain unmodified.

The principle of the method is composed in two parts: the first of them is the fractioning of the pump pulses into multiple replicas at distinct optical frequencies, each of them suitably shifted in time, as described in Fig. 1. The second part corresponds to the generation of a matching multi-frequency probe signal, as it will be described below in this section. Figure 1 schematically illustrates the first part of the principle, in which the light from an optical source composed of several frequency components is used to generate a high-power optical pulse. The purpose is to spread the pulse power among multiple frequency components in order to increase the total pump power launched into the fiber, while keeping the power of each individual pulse below the onset of nonlinear effects [3-5].
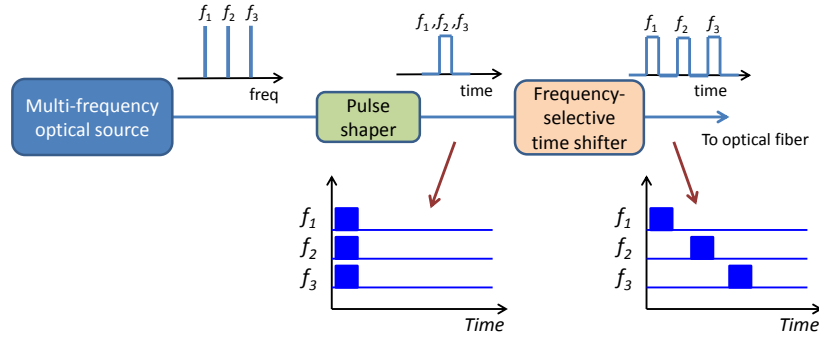

Fig. 1. Schematic showing the principle of the proposed method based on frequency and time multiplexing of the pump signal in Brillouin distributed optical fiber sensors.

Based on the analysis presented in [17,18], it is worth pointing out that if the high-power pulse replicas at different frequencies are launched simultaneously into the fiber, their nonlinear parametric interaction during propagation will mutually seed unwanted nonlinear processes, such as modulations instability [3,4] or four-wave mixing [17]. This cross-interaction will be consequently observed at a reduced power and will also lead to strong distortion in the traces, impairing significantly the system performance. In order to maximize the peak pump power and to avoid nonlinear cross-interactions among the different pump spectral components, a sequential pumping scheme, as the one proposed in [18], has to be employed. This means that the pump pulse replicas at distinct frequencies have to be selectively and distinctively delayed to ideally suppress any temporal overlapping. This wavelength-dependent delay must be at least equal to the single pulse duration to secure that pulses do not overlap in time and location anywhere along the fiber [18]. This also results in the highest optimized peak pump power. The total signal power supported by the fiber can thus be multiplied by an integer factor equal to the number N of frequency components, although each pulse is still limited by the onset of nonlinear effects. Note that the delay between pulses can possibly be reduced below the pulse duration as long as the nonlinear interaction between pulses shows no observable effect.

A matching multi-frequency probe signal can be simultaneously generated from the same multi-frequency optical source depicted in Fig. 1. Two probe sidebands can be symmetrically generated from each pump spectral component by simple amplitude modulation [20] (similar to a standard BOTDA scheme), as schematically shown in Fig. 2. The frequency offset between the N interacting probe-pump pairs remains securely identical, thus evenly increasing the Brillouin interaction and the sensor response by a factor N. Consequently, the total probe power allowed in the fiber can be safely multiplied by a factor N, while each line is still limited at ~5 mW to avoid depletion due to amplified spontaneous Brillouin scattering and

maintain the small gain operation regime [5]. However, a smart choice of the frequency allocation must be made to avoid jamming coincidental Brillouin interactions with other frequency components. This way each of the N pump pulse replica interacts with a single pair of probe components symmetrically centered on the respective pump spectral line.

The method can be interpreted as a spectral parallelization of the Brillouin interaction occurring along the distributed sensor. Since the use of N spectral components gives rise to N independent pump-probe Brillouin interactions, the measured signal amplitude (proportional to the sensor response [2]) will result N-times larger than the one obtained in the standard BOTDA scheme. However, the SNR enhancement provided by the method would certainly depend on the kind of noise dominating the system. For instance, in an optimized photo-detection stage a high trans-impedance amplifier is typically required to improve the electrical SNR, so that the saturation level of the electrical output is generally reached before shot noise dominates (especially in photo-detectors with bandwidths up to 100 MHz as generally employed in BOTDA systems with meter-scale resolution). Under this condition the system is dominated by thermal noise, which is independent of the optical power reaching the photo-detector [21]; and therefore, the proposed technique would show a SNR enhancement proportional to N. However, if a low trans-impedance is used, a higher power reaching the photo-detection would eventually increase the shot noise in the receiver [21]; so that in a shot-noise limited system the expected SNR enhancement provided by the method should increase with a factor proportional to $\sqrt{N}$ instead of N. The situation is actually much different in most of long-range BOTDA systems, since an erbium-doped fiber amplifier (EDFA) is generally inserted in the receiver front-end to increase the power reaching the photo-detector. In such a situation the BOTDA sensor turns out to be essentially dominated by the signal-spontaneous beat noise [21,22], which depends on the amplified spontaneous emission (ASE) noise introduced by the amplifier. Under this condition the SNR of the temporal traces can be written as [21,22]:

$$SNR(z) = \frac{\Delta I_s(z)}{\sigma_{i_{s-sp}}} = \frac{\Delta I_s(z)}{\sqrt{2 I_{ASE} I_s B_e / B_o}} \qquad (1)$$

where $\Delta I_s(z)$, I_s and I_{ASE} are respectively the photocurrents resulting from the sensor response, probe power reaching the receiver and the ASE noise introduced by the EDFA; while B_e and B_o are the electrical bandwidth of the photo-detection and the optical bandwidth of the ASE noise reaching the detector, respectively. Although the use of N tones increases the sensor response and the probe power reaching the detector, the amount of ASE noise also depends on the input power of the EDFA; and therefore, the use of a large number of tones can eventually reduce the noise introduced by the amplifier, resulting in an additional benefit for the proposed method. Although the introduced ASE noise power depends on the specific parameters of the amplifier (e.g. gain, saturation power, and noise figure), the above-described behavior would be expected in most of long-range BOTDA sensors, in which a low probe power typically reaches the receiver front-end.
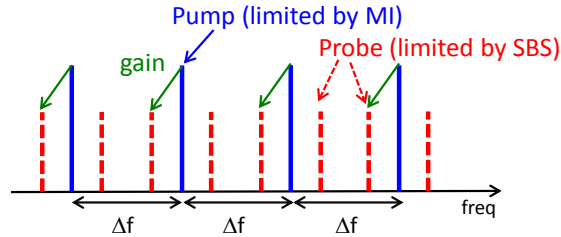

Fig. 2. Spectral allocation of the multi-frequency probe (dashed red lines) and pump (straight blue lines) signals in the proposed method. While the total pump and probe powers can be increased by a factor N (equal to the number of spectral components) to exceed the nonlinear threshold levels, the power of individual lines is still limited by the onset of nonlinear effects.

Additionally, the method also requires a temporal realignment of the generated BOTDA traces reaching the receiver front-end, as schematically illustrated in Fig. 3. Note that the delay between the *N* pulse replicas is expected to generate independent and delayed BOTDA traces over *N* different probe spectral components. In order to avoid temporal jamming due to this de-synchronization, the *N* probe signals containing the Brillouin gain information have to be properly rearranged in time before the photo-detection by applying a reverse delay to the one originally set to the corresponding pump pulse replicas. Actually, this temporal realignment of the *N* BOTDA traces (carried by the probe components) is essential to avoid ruining the spatial resolution of the sensor. Although this second temporal shift is preferably performed optically before photo-detection, following a scheme identical to the one used for the wavelength-dependent delaying on the pump pulse replicas, it can be also carried out in the electrical domain or using signal processing after photo-detection, as proposed in [18].
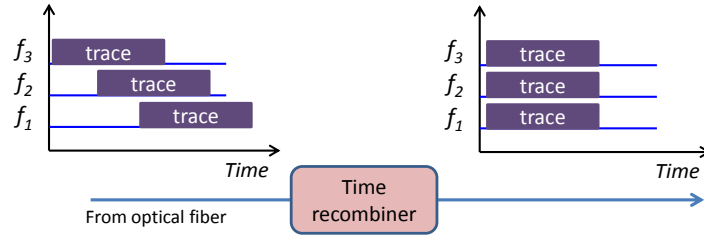

Fig. 3. Temporal realignment of BOTDA traces required at the receiver stage.

The use of multiple spectral components increases the sensor response and SNR of the measurements; however, the scalability of the method is essentially limited by two potential effects: *i)* four-wave mixing between the probe components and *ii)* chromatic dispersion. Due to the close frequency spacing of the multiple tones used in the system, the efficiency of four-wave mixing can quickly increase with the number of tones *N*; however, its impact can be substantially reduced using unequally-spaced spectral components. Since each pump-probe pair interaction is independent from each other, the use of unequal frequency spacing will not have any detrimental impact on the principle of the method. Actually, the use of unequal spacing has been successfully demonstrated in [17,18], where up to $N = 20$ tones of 6.5 dBm and separated by only a few hundreds MHz have been used, resulting in negligible four-wave mixing [17]. On the other hand, the use of a wide spectral range for the multi-frequency pump would certainly lead to chromatic dispersion effects, having a detrimental impact on the spatial resolution. Note that dispersion would affect the pump pulses and also the counter-propagating sensor response so that, considering a round-trip propagation along the fiber, the increment in the spatial resolution at the end of the time-domain BOTDA traces can be written as:

$$\delta z = \frac{\lambda^2}{n} D \cdot (N-1) \cdot \Delta f \cdot L \qquad (2)$$

where λ is the central wavelength of the frequency comb, *n* is the refractive index of the fiber, $D(\lambda)$ is the chromatic dispersion of the fiber at the central wavelength λ, Δf is the frequency spacing between pump components, *N* is the number of spectral components, and *L* is the sensing fiber length. Using Eq. (2) the maximum number of spectral tones *N* can be calculated for the maximum level of error δz tolerated in the system: for instance, using tones separated by $\Delta f = 15$ GHz to interrogate a BOTDA sensor along a 50 km-long standard SMF at 1550 nm ($D = 17$ ps/km·nm), a maximum of $N = 6$ tones can be used to keep the detrimental impact of dispersion on the spatial resolution below 10 cm at the far end of the sensing fiber (thus, representing less than 10% error in the spatial resolution of a sensor with metric resolution). This level of error is generally tolerated in a long-range BOTDA sensor, representing no big

penalty to the system. However, allocating the tones using a more spectrally efficient scheme, the number of components N can be significantly increased, as it will be described below.

Pump and probe frequency components can be spectrally allocated following different possible configurations, with the only requirement that probe sidebands generated around a given pump component do not overlap with other pump/probe spectral lines. Figure 4 describes three possible allocations of the spectral components:
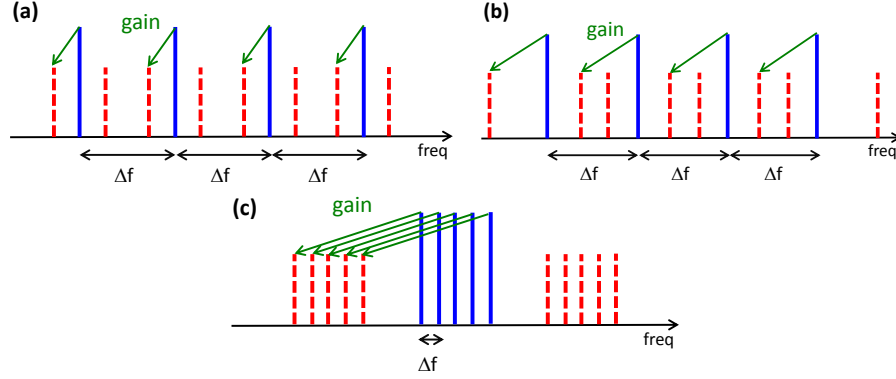

Fig. 4. Possible spectral allocation of pump and probe signals to implement the technique in a BOTDA sensor. The straight blue lines represent the frequency components of the pump, and the dashed red lines represent the counter-propagating probe components. (a) $\Delta f > 2\nu_B$, (b) $\nu_B < \Delta f < 2\nu_B$, and (c) $2\Delta\nu_B < \Delta f < \nu_B$, $\nu_B \approx$ 10-11 GHz being the Brillouin frequency in standard single-mode fibers, and $\Delta\nu_B \approx$ 30 MHz the Brillouin linewidth.

1. The first case, depicted in Fig. 4(a), shows the most intuitive configuration to replicate spectrally the pump-probe interaction of the standard BOTDA scheme. In this case the spectral separation Δf between the N components has to be at least larger than twice the Brillouin frequency in the fiber ν_B to secure no spectral lines overlapping, i.e. $\Delta f > 2\nu_B$ ($\nu_B \approx$ 10-11 GHz in standard single-mode fibers). The main drawback of this configuration is the broad total spectral coverage in presence of a large number N of well separated frequency components: in this case the measured Brillouin gain spectrum is broadened [15,16,23] as a result of the pump wavelength dependence of the Brillouin frequency, while the system also becomes much more susceptible to effects of chromatic dispersion. Dispersion actually imposes the most restrictive limitation to the number of tones in this case, so that the detrimental effect of gain broadening [2,23] can be generally neglected. This is because under a limited number of components (e.g. $N < 20$, $\Delta f = 30$ GHz), the frequency uncertainty induced by gain broadening [2] can be easily overcompensated by the enhancement in the sensor response provided by the N probe-pump interactions [23].
2. The second case is shown in Fig. 4(b), in which the pump-probe pairs are interleaved, so that the frequency separation Δf fulfils the condition $\nu_B < \Delta f < 2\nu_B$, ensuring that the interactions generated by distinct pump components are not competing on the same probe line. This configuration is actually more spectrally efficient than the previous one, mitigating the effects of the gain spectral broadening [2,23] and chromatic dispersion; however, it might require narrower optical filtering at the receiver.
3. Finally, Fig. 4(c) shows a third configuration in which the frequency separation is lower than the Brillouin frequency ν_B but larger than the twice the natural Brillouin linewidth $2\Delta\nu_B \approx 60$ MHz (thus avoiding any possible crosstalk originated from coincidental pump-probe gain interactions [18]); i.e. $2\Delta\nu_B < \Delta f < \nu_B$. Although the multi-line pump could be easier to generate in this configuration since it requires lower frequencies, the scheme may be practically difficult to implement if optical filters are used to separate and to delay

the different N probe components. It may eventually require additional signal processing to reconstruct the BOTDA traces or more sophisticated filtering techniques based, for instance, on coherent detection followed by electrical filtering. In this case the impact of chromatic dispersion turns out to be negligible (even for some hundreds km of sensing range), while the number of spectral lines is ultimately limited by the spectral separation Δf and the Brillouin frequency v_B of the fiber, so that $N < v_B/\Delta f$. Thus, many tens of tones separated by a few hundreds MHz could be employed (e.g. up to N=43 tones separated by $\Delta f = 250$ MHz can be used, assuming a typical Brillouin frequency of $v_B = 10.8$ GHz).

3. Experimental setup

The benefits of the proposed technique are verified using the proof-of-concept setup illustrated in Fig. 5. A comb with $N=3$ spectral components is implemented and generated by externally modulating the intensity of a single-wavelength distributed-feedback laser using a Mach-Zehnder modulator (MZM) driven by a microwave signal at $\Delta f = 17$ GHz. The DC bias voltage of the modulator has been adjusted, so that three spectral lines (carrier and first-order sidebands) are obtained with the same amplitude. Each pump and probe component can then be adjusted to optimal power levels at the sensing fiber inputs. The generated 3-line frequency comb is split into two branches to generate pump and probe waves using the standard methods employed in basic BOTDA systems.
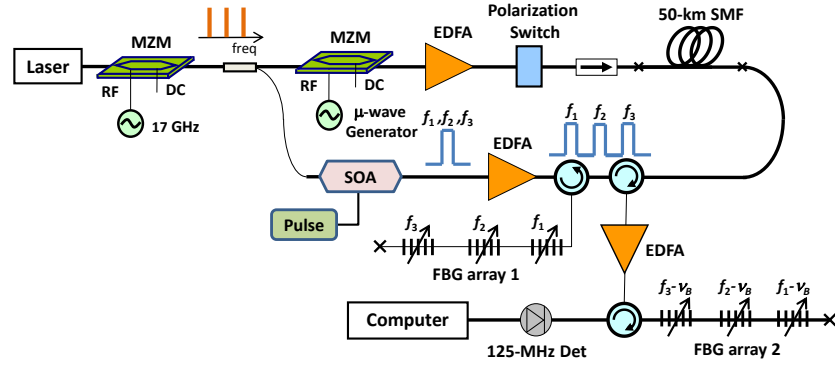

Fig. 5. Experimental setup for the proposed BOTDA sensor based on multi-frequency time-shifted pump pulses. The scheme uses $N=3$ frequency components, separated by $\Delta f = 17$ GHz. The first array of FBGs applies a frequency-dependent delay to the distinct pump frequency components, denoted as f_1, f_2 and f_3. In the receiver, the distinct BOTDA trace components are temporarily rearranged by a second array of FBGs; each of them tuned, in reverse order, to the lower-frequency probe components f_3-v_B, f_2-v_B and f_1-v_B (being v_B the average Brillouin frequency of the fiber).

The probe light is created using a MZM operating in carrier-suppression mode [20], giving rise to 3 pairs of sidebands centered on the original $N=3$ comb frequencies, so that a total of 6 spectral lines are obtained for the probe. Since the frequency spacing of the comb is $\Delta f = 17$ GHz, the probe sidebands generated from each pump component are interleaved as described in Fig. 4(b). A polarization switch is used to prevent any gain fading resulting from the polarization-dependent Brillouin gain. Meanwhile, pump pulses are created with high extinction ratio by a semiconductor optical amplifier (SOA), in which the gain is gated to obtain a 20 ns-long optical pulse, corresponding to a 2 m spatial resolution. Adjusting the output power of the EDFAs, probe and pump powers are separately optimized at the fiber input to maximize the sensor response and avoid nonlinear effects.

In this implementation, the delay between different frequency components (for the pulsed pump in the transmitter and probe signal in the receiver) is carried out by arrays of cascaded fiber Bragg gratings (FBGs), each grating being tuned at one of the different frequency

component of the optical comb. Using an optical circulator, the multi-frequency pump pulse is sent into a first array of three 7 cm-long FBGs, having central wavelength at 1551.1 nm (at room temperature and zero strain), transmission band of 43 pm full-width at half-maximum (FWHM), high reflectivity (higher than 90%), and positioned every 5 m along the fiber. Each FBG has been mounted on a distinct translation stage for a wavelength-selective fine tuning on the $N=3$ distinct comb frequencies delivered by the first MZM. Thus, by simply adjusting the reflection band of the FBGs, three pulses spectrally spaced by $\Delta f = 17$ GHz are obtained with a temporal separation of 50 ns.

Pump and probe components are launched into a 50 km-long standard single-mode fiber (SMF). At the receiver, the multi-frequency probe is first amplified by an EDFA, and then sent into a second array of FBGs having the same characteristics as the first array. The reflection band of each FBG is properly tuned in order to apply a selective reverse delay to the probe components, so that the time differences resulting from the delayed pump pulses are exactly compensated, following the principle described in Fig. 3. This way BOTDA traces are automatically rearranged in time to eventually obtain the equivalent trace corresponding to the summed N pump-probe interactions. In addition to the delay provided by this second array of FBGs, each FBG also filters out one sideband in each pair (for instance the upper sideband experiencing Brillouin loss and showing a cancelling negative response) as well as the ASE noise originated by the EDFA. The multi-frequency probe signal containing the rearranged Brillouin gain information is detected by a 125 MHz photo-detector, and then digitalized with an acquisition card connected to a computer.

4. Experimental results and discussion

To experimentally validate the proposed method, BOTDA traces at the peak gain frequency have been acquired for both $N=3$ and $N=1$ (standard case). The peak power of the each pump pulse replica has been adjusted to the maximum of 100 mW to avoid modulation instability [3,4], so that the total pump power is 300 mW for $N=3$. The three pulses are properly ordered in time and frequency domains to avoid nonlinearities, as formerly described.
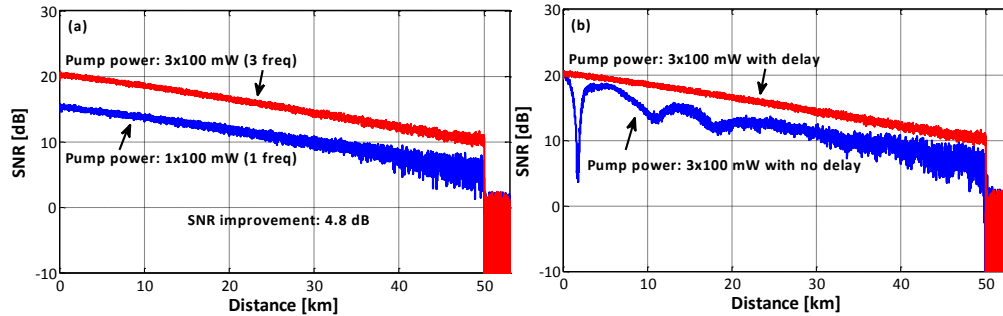

Fig. 6. Signal-to-noise ratio (SNR) measured at the peak gain frequency. (a) Comparison between the standard BOTDA ($N=1$) and the proposed scheme using $N=3$ spectral components and delayed pump pulses. (b) SNR and sensor response evolution along the fiber, measured with $N=3$ components, with (red curve) and without (blue curve) delay between pump pulses.

Figure 6(a) compares the SNR of the BOTDA traces for both cases, indicating that the use of $N=3$ frequency components enhances the sensor response [2] and thus the SNR of the measurements by a factor 3, corresponding to 4.8 dB. Using the standard scheme ($N=1$) with a 2 m spatial resolution and 2000 time-averaged traces, a SNR equal to 6.1 dB is experimentally observed at the fiber far end. However, using $N=3$ components, the SNR has been improved up to 10.9 dB under the same condition. It is important to mention that a photo-detector with a high trans-impedance amplifier has been used to optimize the SNR of the BOTDA traces; thus, making the system dominated by thermal noise. This has been experimentally verified by measuring the noise power after photo-detection and by calculating the standard deviation

of the measured temporal traces after the end of the fiber (i.e. in absence of Brillouin gain) when using $N = 1$ and $N = 3$ tones. A standard deviation equal to 41.5 µV (after 2000 averages) has been obtained from the BOTDA traces in both cases, being exactly the same level as the one obtained with the same number of averages when no light enters the photo-detector. This result points out that total noise in the BOTDA system is the same for $N = 1$ and $N = 3$ and turns out to be equal to the thermal noise of the photo-detector. This explains the SNR enhancement equal to $N = 3$ (i.e. 4.8 dB) obtained in the experiment and shown in Fig. 6.

It is worth pointing out that no distortion (potentially originating from nonlinear effects) is observed in the BOTDA traces measured with $N=3$ (red curves in Fig. 6), even though high pump power (300 mW) is launched into the fiber. Actually the delay between pulses at different frequencies plays a crucial role in the method: if the three 100 mW pulses at distinct frequencies are simultaneously launched into the fiber with no delay, the parametric interaction among the spectral components leads to distorted traces. Figure 6(b) actually compares the SNR of the BOTDA traces obtained at the peak gain with (red curve) and without (blue curve) delay between pulses. Interestingly, the same sensor response and SNR are observed in both cases near the fiber input (due to the same input pump power); however, when no delay is applied, nonlinearities resulting from parametric interaction among pulse frequency components produce strong oscillations in the effective pump power [4,17] and hence in the measured Brillouin gain. However, these oscillations are completely eliminated by temporally shifting the pump pulse replicas at the $N=3$ different frequencies, leading to a perfect trace (red curve) in Fig. 6(b) with no distortion. This demonstrates that the delay of the multiple copies of the pump pulse is essential to avoid nonlinearities resulting from the interaction of high-power overlapping pulses inside the fiber. It has also been experimentally demonstrated that the proposed method does not increase the amount of pump depletion, even though higher probe power is used. In this case residual pump depletion (after propagation along the 50 km of fiber) has been measured to remain below 4%, resulting in negligible biasing effect and minimum trace distortion [5].

Figure 7 shows the Brillouin gain spectrum versus distance, measured using a frequency scanning step of 1 MHz and $N=3$ spectral components. The Brillouin frequency profile is obtained after fitting the measured spectrum with a parabolic curve [2], as shown in Fig. 7 inset. Calculating the standard deviation of the measured Brillouin frequency along the fiber, the final uncertainty on the sensor response has been estimated for the standard BOTDA configuration ($N=1$) and for the scheme using $N=3$ spectral components [2].
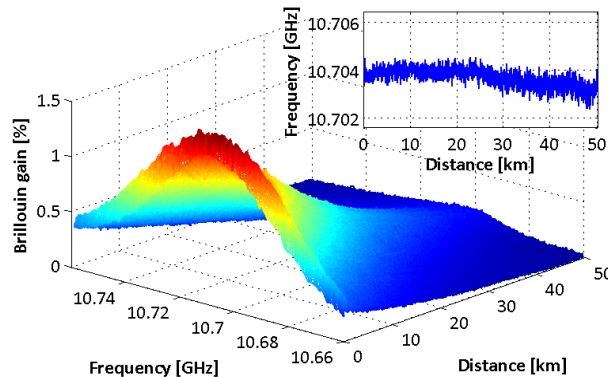

Fig. 7. Measured Brillouin gain spectrum versus distance obtained using $N=3$ components. Inset: Calculated Brillouin frequency profile at ambient temperature (24°C).

Figure 8 shows the frequency uncertainty versus distance for both analyzed cases, indicating that the accuracy of 1.8 MHz – obtained with the standard scheme at a distance of 50 km – can be improved down to 0.6 MHz using the proposed method with $N=3$. This

corresponds to a frequency uncertainty improvement equal to a factor 3, being in perfect agreement with the prediction expected from the 4.8 dB SNR enhancement [2].
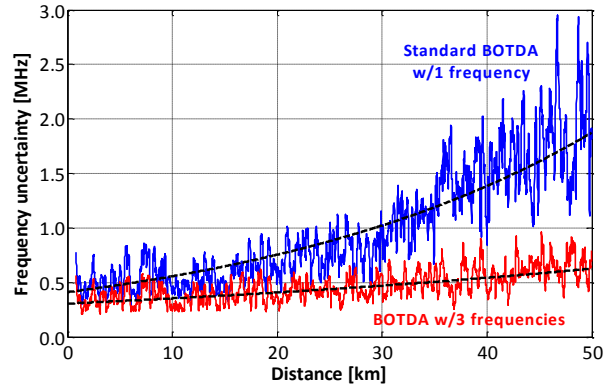

Fig. 8. Frequency uncertainty versus distance, for BOTDA schemes using N=1 (standard) and N=3 spectral components, along a 50 km-long standard single-mode fiber using 2 m spatial resolution and 2000 time-averaged traces. The frequency uncertainty is here calculated as one standard deviation of the Brillouin frequency measured at each fiber location.

Finally, the spatial resolution of the method has been experimentally verified. For this purpose, 2 m of the sensing fiber close to the fiber far end have been heated up to 50°C, while the rest of the fiber is kept at ambient temperature (24°C). Considering that the method requires a pulse de-synchronization followed by a suitable re-synchronization of the temporal traces, a hot-spot detection is actually a crucial test for the proposed technique. Possible imprecisions in the reverse delays delivered by the second FBG array will certainly jam the spatial information contained in the N delayed temporal traces, resulting in a detrimental impact on the spatial resolution. Figure 9 shows the hot-spot measured at a ~50 km distance using the proposed technique with N=3 frequencies. Experimental results indicate a correct determination of the temperature within the hot region and no penalty on the 2.0 m spatial resolution is observed using the 20 ns de-synchronized pump pulses.
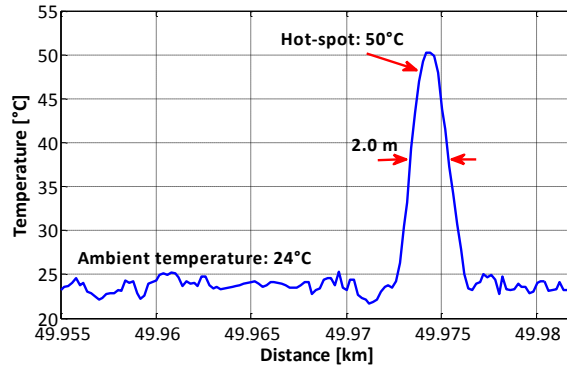

Fig. 9. Hot-spot detection near the fiber far end (~50 km distance), demonstrating 2 m spatial resolution.

4. Conclusion

A technique to enhance the response and performance of BOTDA sensors has been proposed and experimentally validated. The method is based on a frequency comb and a wavelength-dependent temporal shift of pump pulses, providing an elegant method to by-pass the fundamental limits imposed by detrimental nonlinear effects. This requires a re-

synchronization of the corresponding BOTDA traces. Consequently, the sensor response can be multiplied by integer steps, depending on the number N of frequency components, while the implementation is partially limited by the added complexity of the passive time-frequency mux-demux units. The additional SNR provided by the method is crucial to extend the sensing range, to reduce measurement time, and/or to improve spatial and measurand resolutions. Compared to alternative approaches, the technique also offers many advantages: simple direct detection can still be employed, avoiding sophisticated detection schemes based, for instance, on coherent detection. Furthermore, the frequency scan, acquisition procedure and data processing remain identical to the basic BOTDA scheme.

The configuration presented here as a proof of concept, based on FBGs arrays, is certainly not the only possible implementation of the method and schemes using more advanced devices with better intrinsic stability are under consideration. It is possible to envisage that the sensor response and SNR enhancement provided by the method could be increased with a larger number of frequency components: this is particularly beneficial for very long sensing ranges, where low power levels are expected at the receiver front-end. It is important to point out that the maximum number of spectral components is essentially limited by chromatic dispersion when a broad spectral range is covered by the frequency comb. However, the detrimental effect of dispersion on the spatial resolution can be significantly reduced using a more spectrally efficient scheme, as the one described in Fig. 4(c). Additionally, there could be other more practical limitations: for instance, a large number of components will reduce the power available for each pump and probe component, simply because the optical gain of EDFAs will be shared by several spectral lines. To overcome this limitation and optimize the pump and probe powers, high-power EDFAs or cascaded EDFAs might be required; however under realistic conditions this might bring additional noise to the system reducing the effectiveness of the proposed technique.

It has also to be mentioned that the method can be freely combined with other sophisticated techniques, such as optical pulse coding, coherent detection and distributed Raman amplification, thus providing a further improvement to the sensor performance. For instance, the use of return-to-zero (RZ) pulse coding makes it possible to straightforwardly combine the coding method with the technique proposed here. In order to implement a reliable coded BOTDA system, pulses with RZ and a duty cycle below 20% are typically required to avoid effects resulting from a pre-activated acoustic wave. So, by simply interleaving N shifted replicas of the pump pulses in between two consecutive bits of the code, long code sequences can be used along with the proposed method. For instance, a duty cycle of 20% would allow the use of $N=5$ frequency components with interleaved pulses; the only requirement is that the pulse separation in the code should be greater than N-times the pulse width to avoid temporal overlapping between code replicas at different frequencies. Note that this is possible because each pulse replica (at different frequency component) generates an independent acoustic wave, so that no Brillouin interaction is expected between two consecutive pulses at different frequencies, even if they are separated by less that the acoustic wave response time. This implementation will be possible independent of the number of bits in the code.

Acknowledgments